Plasma Polymerization of Hexafluoropropylene: Film Deposition and Structure

R. CHEN, V. GORELIK, and M. S. SILVERSTEIN*

Department of Materials Engineering, Technion-Israel Institute of Technology, Haifa 32000, Israel

SYNOPSIS

Thin, pinhole-free, highly adhering films for advanced technology applications can be deposited through plasma polymerization, a low temperature, solvent-free process. This research studies the influence of plasma environment (power, pressure, and monomer mass flow rate (F_m)) on the plasma polymerization of hexafluoropropylene (HFP) using a common industrial parallel-plate plasma reactor. The deposition and structure of the transparent, yellow, and highly adhering plasma polymerized HFP (PPHFP) film are investigated. The rate of polymerization (R_p) increases with power (W) and reaches a plateau when the plasma changes from energy starved to monomer starved while the rate of etching (R_e) continues to increase. The rate of deposition (R_d), the difference between R_p and R_e, increases with W, reaches a maximum, and then decreases. In a monomer starved plasma R_d increases with F_m or pressure through a more efficient utilization of the energy supplied at a given W or even at a given W/F_m. The abstraction of F and the preferential scission of the C—CF_3 bond can explain the F/C ratio of 1.5, the significant amount of double bonds, and the relative lack of CF_3 in a PPHFP that consists of CF_3, CF_2, and CF groups. A gas phase dominated polymerization produces submicrometer particles some of which agglomerate into spheres. Both the particles and the spheres deposit on the surface and are incorporated into the film with further polymerization. © 1995 John Wiley & Sons, Inc.

INTRODUCTION

The use of high performance, high temperature polymer thin films is expanding into many advanced technology applications once associated with ceramic thin films. Thin films for device passivation layers, interlayer dielectrics, planarizing interlayers, and resists are of interest to the microelectronics industry.[1,2] Biocompatible coatings are of interest to the biomedical industry, permselective coatings to the membrane industry, and protective coatings to the aerospace and automotive industries. Thin fluoropolymer films can have many advantages including a low coefficient of friction, a low surface tension, thermal stability, biocompatibility, and chemical resistance. Unfortunately, the techniques used to deposit thin fluoropolymer films can involve etchants, solvents, and temperatures that limit their applicability.

Plasma polymerization is a low temperature (room temperature), solvent-free process that can be used to deposit thin fluoropolymer films from a variety of organic compounds that are not polymerizable by standard techniques.[3-5] The neutral species entering the reactor are fragmented into reactive species as energy is transferred by the electrons in a low temperature, low pressure plasma environment. The substrate molecules are activated by exposure to the plasma environment and chemical bonds are formed with the polymerizing reactive monomer fragments.

The highly adhering, pinhole-free and crosslinked plasma polymerized (PP) films have potential applications in the microelectronics, biomedical, membrane, aerospace, and automotive fields.[6-11] Only a few of the myriad possible applications of PP, and specifically of PP fluoropolymer films, have been studied and developed. Because exposure to a plasma is commonly used for cleaning, planarization,

* To whom correspondence should be addressed.

Journal of Applied Polymer Science, Vol. 56, 615-623 (1995)
 CCC 0021-8995/95/050615-09

etching, and sputter coating, then coating with a PP film might even be effected using a common industrial plasma reactor.

The structure and properties of PP thin films depend on the plasma environment, specifically the pressure (P), monomer mass flow rate (F_m), power (W) and feed composition, all of which interact in a complex manner. The plasma polymerization of fluorocarbons is even more complex than that of hydrocarbons because the rate of the competing plasma etching reaction is more significant. The successful deposition of a PP fluorocarbon film has been associated with two factors. An unsaturated monomer produces difunctional fragments that are more likely to participate in a polymerization reaction than in an etching reaction.[3] A low fluorine to carbon (F/C) ratio in the monomer yields a lower etching rate because the release of atomic F is an important part of the etching mechanism.[12]

Both tetrafluoroethylene (TFE) and hexafluoropropylene (HFP) are unsaturated fluorocarbons with F/C ratios of 2. The PP of HFP ($CF_2{=}CF{-}CF_3$) has not been studied in as great a detail as the PP of TFE ($CF_2{=}CF_2$). The objective of this research is to develop insight into the deposition and structure of PPHFP polymerized under various plasma environments (W, P, F_m) using a common industrial plasma reactor.

EXPERIMENTAL

PP

The central part of the plasma reactor system illustrated schematically in Figure 1 is a parallel-plate electrode radio frequency (13.56 MHz) plasma reactor (March Instruments, Jupiter III). The reactor was evacuated to 2.5 Pa with a vacuum pump (Alcatel AC-2012) and the temperature of the anodized aluminum parallel-plate electrodes was maintained at 20°C with a circulating liquid cooler (Neslab RTE-100). One inlet rotameter was calibrated for HFP (Matheson) while the other inlet rotameter was calibrated for argon. Glass optical microscopy slides were used as substrates and were centered on the bottom electrode.

The following steps were taken in the plasma polymerization process:

1. The substrate was placed on the bottom electrode that was cooled to 20°C. The reactor was evacuated to 5 Pa, purged with argon at 16.9 sccm, and then evacuated to 2.5 Pa.

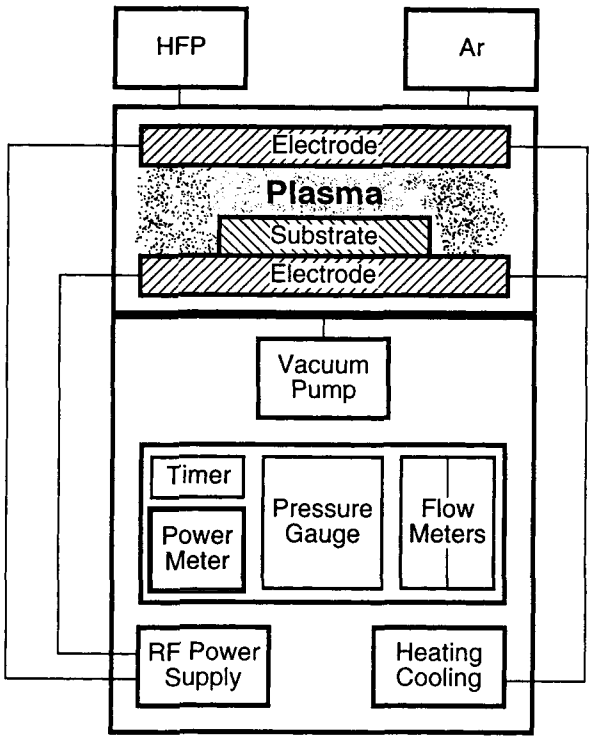

Figure 1 Schematic illustration of the parallel-plate plasma reactor.

2. The substrate was cleaned by exposure for 5 min to an argon plasma at 200 W, 100 Pa, and 16.9 sccm. The reactor was then evacuated to 2.5 Pa.
3. HFP was fed into the reactor at the desired initial pressure (P_0) and F_m. The plasma was ignited at the desired power. The inlet and outlet valves were readjusted if a specific P was desired. The plasma exposure time (t) was 5 min unless stated otherwise.
4. After the plasma was extinguished the reactor was evacuated to 2.5 Pa, purged with argon at 16.9 sccm, and then opened to the atmosphere.

The rate of deposition (R_d) was calculated both on a mass and thickness basis. The mass gained was measured with an accuracy of 0.1 mg (Mettler AE-163 microbalance) yielding the deposition rate in terms of mass per area [g/(m^{2}min)]. The thickness was measured in several different places using a stylus apparatus with an accuracy of 0.05 μm (Tencor α-step-100) yielding an average deposition rate in terms of thickness (μm/min). The experimental conditions under which each plasma parameter was investigated are listed in Table I.

Table I Experimental Conditions

Measured	Varied	Constant
P	W	P_0 = 187 Pa; F_m = 18.3 sccm
R_d	W	P = 187 Pa; F_m = 18.3 sccm; t = 5 min
R_d	F_m	P = 187 Pa; W = 100 W; t = 5 min
R_d	P	F_m = 18.3 sccm; W = 100 W; t = 5 min
R_d	t	F_m = 18.3 sccm; P = 187 Pa; W = 100 W

Polymer Film

The PPHFP characterized in detail was polymerized at 100 W, 187 Pa, 18.3 sccm HFP, and 5 min. The chemical structure of PPHFP was measured using two complementary methods. Electron spectroscopy for chemical analysis (ESCA) was performed on the PPHFP coated slides using an Al $K\alpha$ source (Perkin–Elmer Physical Electronics 555 ESCA/Auger). The atomic concentrations were determined with an accuracy of 1% in a low resolution scan and the nature of the bonds with carbon in a high resolution C_{1s} scan. Transmission Fourier transform infrared spectroscopy (FTIR) (Unicam Mattson 1000 FTIR) provided chemical information that reflects the bulk PPHFP more accurately than the surface specific ESCA. The PPHFP films for FTIR characterization were separated from the substrates by soaking in acetone overnight and drying at room temperature for several days.

The topography of the PPHFP films were examined in both reflection optical microscopy (ROM) (Zeiss Axiophot) and scanning electron microscopy (SEM) (JEOL JSM-840). The PPHFP films were coated with a 0.05-μm layer of evaporated gold before entering the SEM.

RESULTS AND DISCUSSION

HFP Polymerization and Plasma Power

The influence of plasma power on the polymerization rate (R_p) was investigated through the change in pressure following plasma ignition. The reactor chamber was held at a given P_0 and F_m, the plasma ignited at the desired power, and the change of pressure observed. Immediately on plasma ignition there was a small increase in pressure with HFP fragmentation because the number of particles in the gas phase rose. The pressure increase was brief and was followed by a pressure decrease with conversion of monomer to polymer because the number of particles in the gas phase was reduced. The steady-state pressure reached in less than 1 min indicates that steady-state polymerization has been achieved. At a constant F_m, R_p is related to the extent of monomer to polymer conversion as seen in the decrease in pressure.

The effect of plasma power on steady-state pressure, and thus on steady-state polymerization, is seen in Figure 2 (constant F_m). The pressure decreases with power until a pressure plateau is reached. At low powers the plasma is energy starved and an increase in power increases monomer conversion to polymer. A pressure plateau is reached when the plasma is monomer starved and further

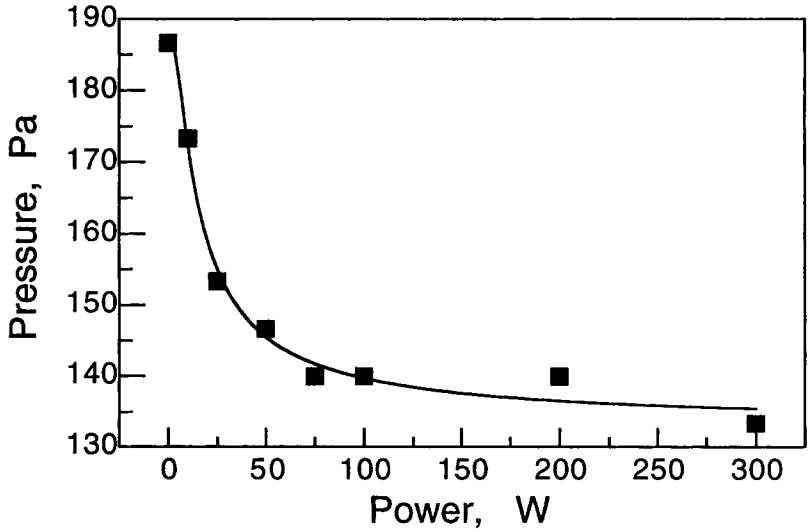

Figure 2 The influence of plasma power on pressure (18.3 sccm).

increases in power do not increase monomer consumption. R_p, from the change in the slope with power in Figure 2, increases rapidly at low powers and then reaches a plateau. The power at which R_p reaches the plateau is the critical power (W_c) and indicates when the energy starved plasma becomes a monomer starved plasma (for that F_m). The W_c estimated from the pressure plateau in Figure 2 lies between 50 and 75 W.

PPHFP Deposition

Plasma Power

The plasma polymerization of HFP was investigated at 187 Pa and 18.3 sccm, well within the range of conditions that provide a stable plasma environment. A transparent, yellow, and highly adhering film is formed on a glass substrate exposed to an HFP plasma for 5 min. The complex variation of R_d with power is seen in Figure 3 (constant P, F_m). At low powers the polymerization reaction is energy starved and increasing power rapidly increases polymerization and thus deposition. R_d eventually reaches a maximum and begins to decrease because the significant etching rate (R_e) in fluorocarbon plasmas also increases with power. R_d is the difference between R_p and R_e, with $R_p > R_e$. The maximum in R_d at 50 W in Figure 3 results from the variation of R_p and R_e with power. At high powers R_p reaches a plateau while R_e continues to increase thus yielding a continuously decreasing R_d.

Monomer Supply

The effect of monomer supply on a monomer starved HFP plasma was investigated at a power of 100 W (100 W > W_c for the F_m studied). There is a relatively linear relationship between R_d and F_m in Figure 4 (constant P, W). The increase in F_m yields an increase in the number of monomer molecules exposed to the plasma environment and an increase in the number of reactive molecules that encounter the substrate surface. As the plasma is monomer starved ($W > W_c$) the energy supplied is used more efficiently with the addition of monomer yielding the increase in R_d. This type of relationship between R_d and F_m would not occur in an energy starved plasma ($W < W_c$). The decrease in residence time that results from an increase in F_m becomes a more significant factor with $W < W_c$ and increasing F_m could even yield a decrease in R_d.

The ratio of plasma power to mass flow rate (W/F_m) is used to describe the energy per mass monomer.[3] W/F_m does describe the plasma environment more accurately than simply plasma power but does not yield a parameter that uniquely describes the plasma environment (pressure, for instance, is not taken into account). Figure 5 shows both Figure 3 and Figure 4 replotted in terms of W/F_m. The curve in Figure 5 showing the variation of R_d with W/F_m at constant F_m is, of course, identical to that showing the variation of R_d with power in Figure 3. R_d increases at low W/F_m, decreases at high W/F_m, and has a maximum at 25 MJ/kg because R_p reaches a plateau at a critical W/F_m [$(W/F_m)_c$].

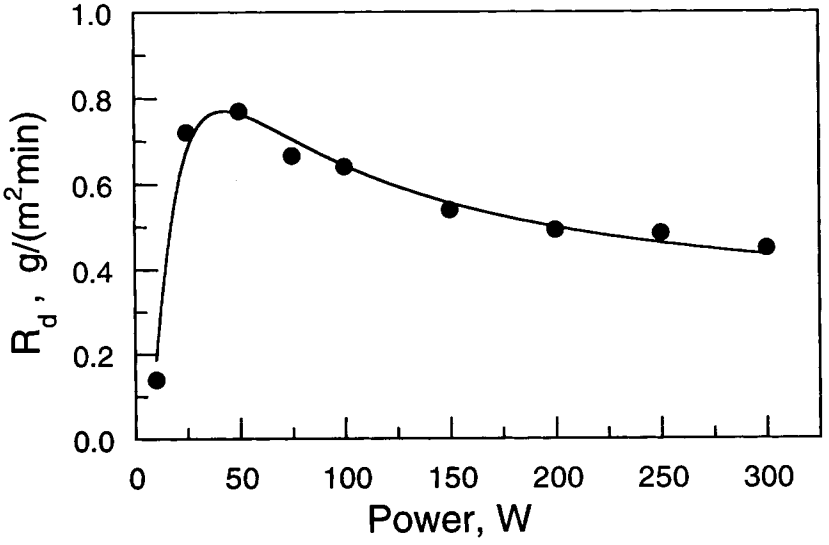

Figure 3 The influence of plasma power on R_d (18.3 sccm, 187 Pa).

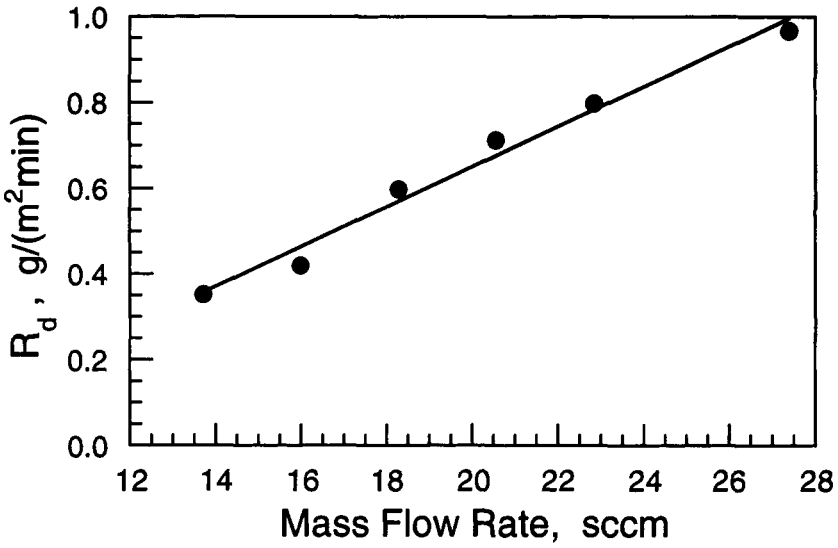

Figure 4 The influence of F_m on R_d (100 W, 187 Pa).

The curve in Figure 5 showing the variation of R_d with W/F_m at constant power only represents the situation when W/F_m is greater than $(W/F_m)_c$. R_d is inversely proportional to W/F_m in this curve because R_d is proportional to F_m in Figure 4. The drastically different shapes of the two curves in Figure 5 indicate that even at a constant pressure the parameter W/F_m does not sufficiently describe the plasma environment. Through a comparison of the curves it can be seen that R_d increases with increasing F_m for a given W/F_m.

The relatively linear variation of R_d with pressure in Figure 6 (constant W, F_m) can be described in a similar fashion as the variation of R_d with F_m in Figure 4. Increasing the pressure at a given F_m increases the concentration of monomer in the reactor. As the plasma is monomer starved ($W > W_c$) the energy supplied is used more efficiently with the addition of monomer yielding the increase in R_d. In addition, the generation of atomic F, hence R_e, has been observed to be inversely proportional to pressure.[13] The generation of polymerizing fragments, hence R_p, has been observed to be proportional to pressure. Increasing the pressure shifts the balance between the competing reactions in favor of polymerization and R_d increases. Here again the effect

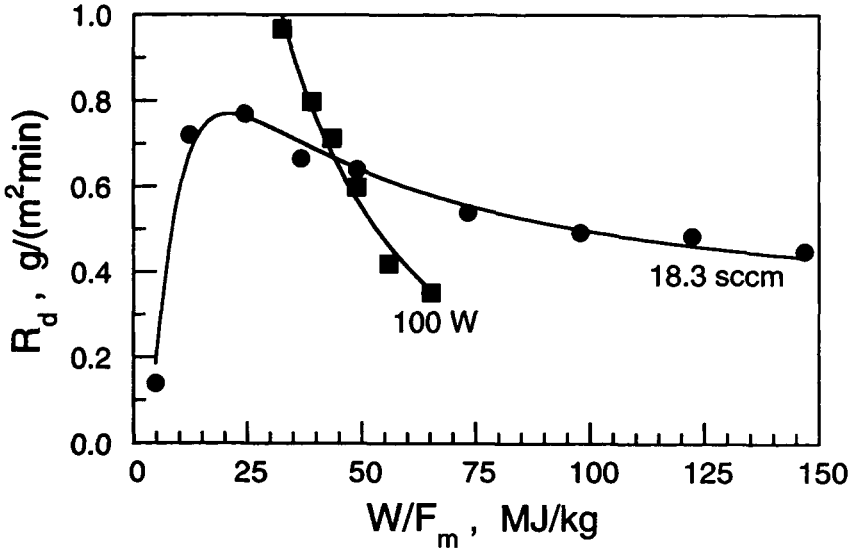

Figure 5 The influence of W/F_m on R_d (187 Pa). (●) 18.3 sccm, from Figure 3; (■) 100 W, from Figure 4.

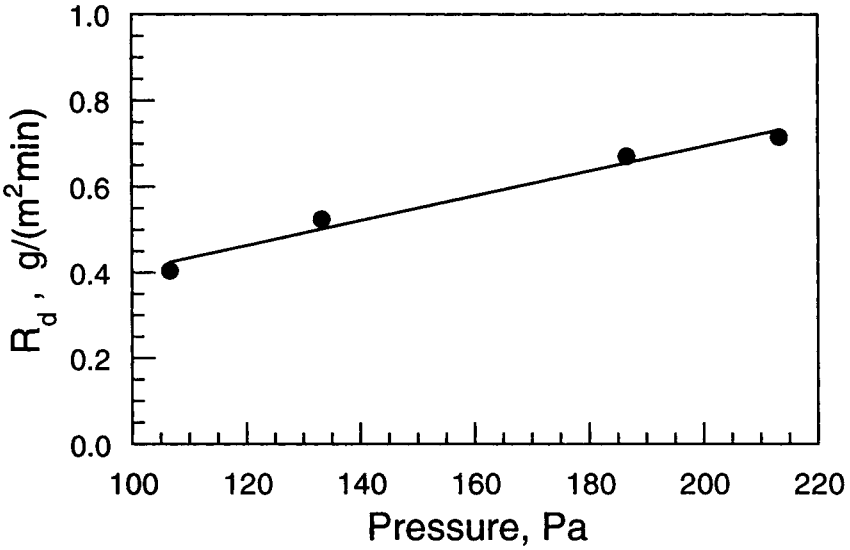

Figure 6 The influence of pressure on R_d (100 W, 18.3 sccm).

of an increase in pressure on R_d may be different in an energy starved ($W < W_c$) plasma.

PPHFP Film

The PPHFP characterized in detail was polymerized at 100 W, 187 Pa, and 18.3 sccm HFP ($W > W_c$). Plasma exposure time has little effect on R_d, as seen from the linear variation of deposition with time in Figure 7. The R_d calculated from the slopes in Figure 7 are 0.77 g/(m^2 min) through mass measurements or 0.35 μm/min through thickness measurements. The ratio of the two deposition rates yields a PPHFP density of 2.2 g/mL. In spite of the differences in structure, the density of the crosslinked amorphous PPHFP is similar to the densities of commercial semicrystalline fluoropolymers such as PTFE and the copolymer of TFE and HFP, fluorinated ethylene-propylene copolymer (FEP).

The crosslinked amorphous nature of PPHFP originates in the random addition of fragments that produces a molecular structure quite different from that of typical polymer repeat units. A PPHFP F/C ratio of 1.5 is revealed through ESCA that found carbon, fluorine, and 1.5% oxygen. The broad PPHFP ESCA C_{1s} spectrum in Figure 8 exhibits CF_3, CF_2, CF, and C—CF bonds and is typical of PP fluorocarbons. The CF_3 peak in Figure 8 is sig-

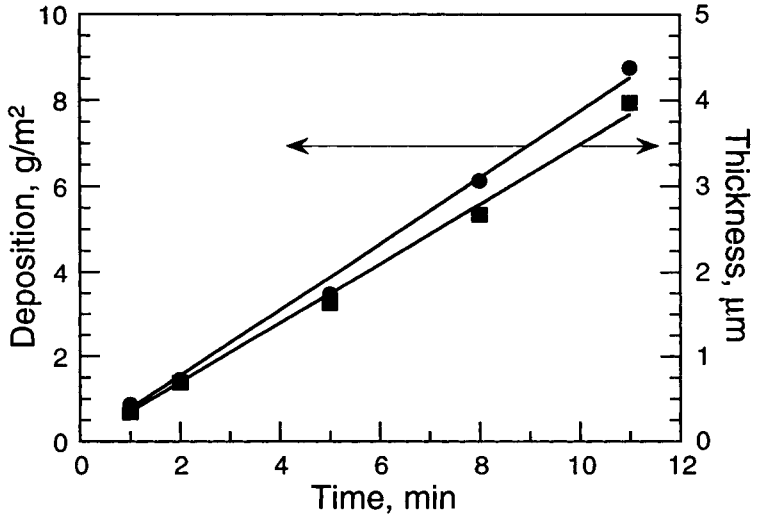

Figure 7 The influence of plasma exposure time on deposition.

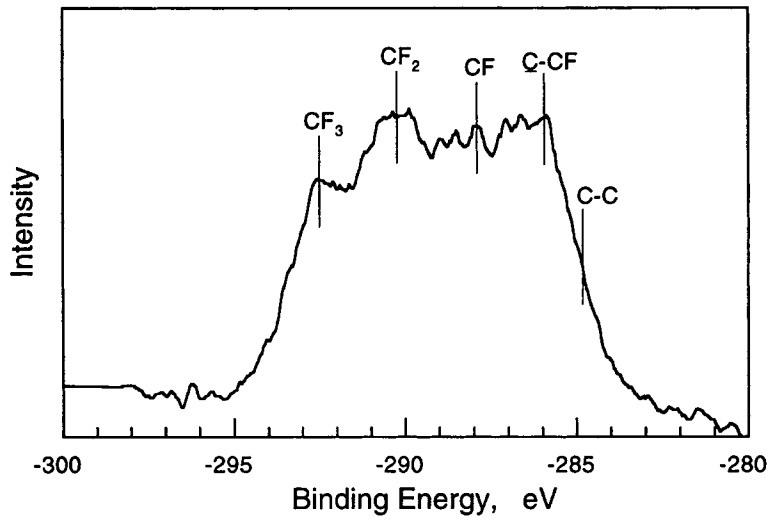

Figure 8 ESCA C_{1s} spectrum of PPHFP.

nificantly smaller than the CF_2 and CF peaks. A CF_3 deficiency in the polymer structure helps explain the F/C ratio of 1.5 in a polymer whose monomer has an F/C ratio of 2 and a $CF_3 : CF_2 : CF$ ratio of 1 : 1 : 1.

The chemical structure is further elucidated through the FTIR spectrum in Figure 9. The wide peak at 1229 cm^{-1} represents CF_3, CF_2, and CF groups as found through ESCA. The peaks at lower wave numbers are also associated with C—F bonds. The peaks at higher wave numbers, however, indicate the presence of double bonds, with 1718 and 1781 cm^{-1} associated with CF=CF and $CF=CF_2$, respectively.

R_e is large enough in the monomer starved conditions under which the PPHFP is synthesized to yield a decrease in R_d and must be considered in the analysis of the polymerization. The etching reaction has been described as involving the release of atomic F and the polymerization reaction as involving CF_x fragments.[14] The CF_2 fragment has been described as the important factor in the determination of R_p with the CF and CF_3 fragments as relatively unimportant.[13] In fact, the CF_3^+ ion has even been described as participating in a physical etching process.[4]

The loss of fluorine originates in the fragmentation of HFP with its F/C ratio of 2 and the generation of fragments that participate in etching but not in polymerization. There are several reactions that can contribute to the lower F/C ratio and the presence of a significant amount of double bonds in

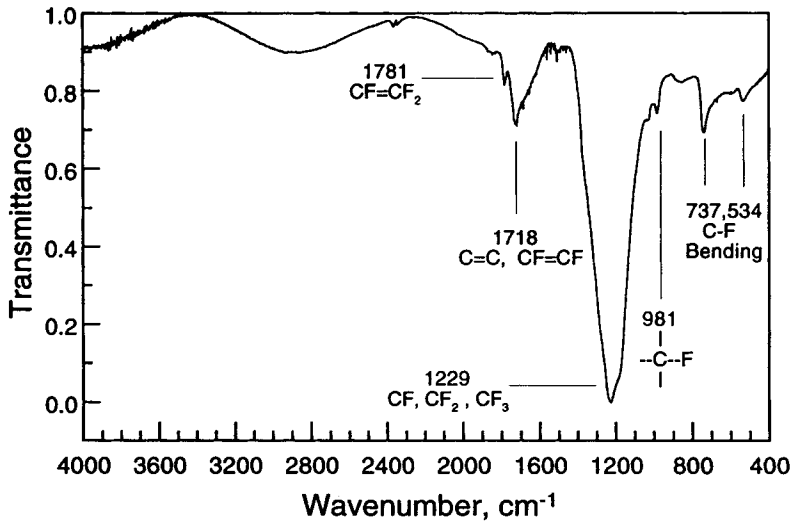

Figure 9 FTIR spectrum of PPHFP.

PPHFP. One reaction is based on the tendency to break the C—F bond that increases with power. Breaking the C—F bond releases atomic F and enhances etching.[3] The atomic F can react with the monomer yielding a polymerizable radical containing a double bond that is then incorporated into the polymer structure.[15]

Another reaction is based on the scission of the C—C bond that is the preferred route for fluorocarbon plasma polymerization.[3] The preferential scission of the $C—CF_3$ bond would release two fragments. The CF_3 fragment would not participate in the polymerization reaction as vigorously as the $CF_2=CF$ fragment with its F/C ratio of 1.5 and double bond. In addition, the possible formation of difluoroacetylene and cyclic compounds in the fluorocarbon plasma would also contribute to the formation of PPHFP with an F/C ratio of 1.5 and a significant amount of double bonds.[16]

The ROM micrograph in Figure 10 reveals that the PPHFP does not form a smooth and uniform film. Spheres approximately 1 μm in diameter are arranged on a relatively flat but grainy surface. These spheres seem to be organized in parallel lines whose origin might lie in the streamlines of the flowing gas. The SEM micrographs in Figure 11 show that these spheres are actually agglomerates of 0.2–0.5 μm particles. The relatively flat grainy surface beneath the spheres is constructed of these same particles.

The submicrometer particles seem to be formed in a gas phase dominated PP. The particles deposit on the surface, undergo further polymerization, and become incorporated into the film structure. Some particles agglomerate within the gas phase and form spheres that are also deposited on the surface and incorporated into the film with further polymerization. This particulate PPHFP topography is far from the smooth uniform thin film sought for advanced technology applications. To shift the reaction from gas phase dominated PP to surface dominated PP changes must be made in the plasma parameters and/or the feed composition. These latter changes might also be used to yield significant variations in the chemical structure of PPHFP.

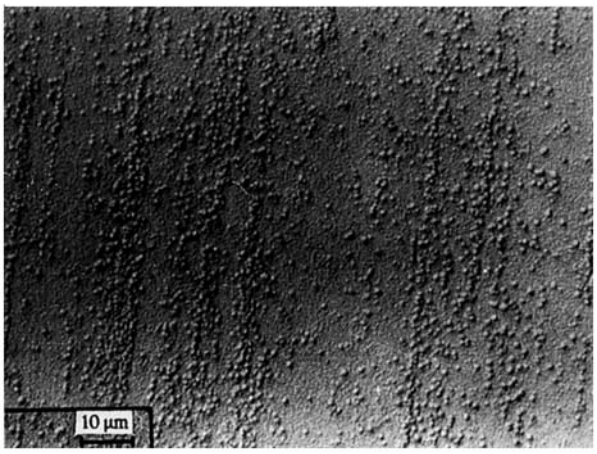

Figure 10 ROM micrograph of PPHFP.

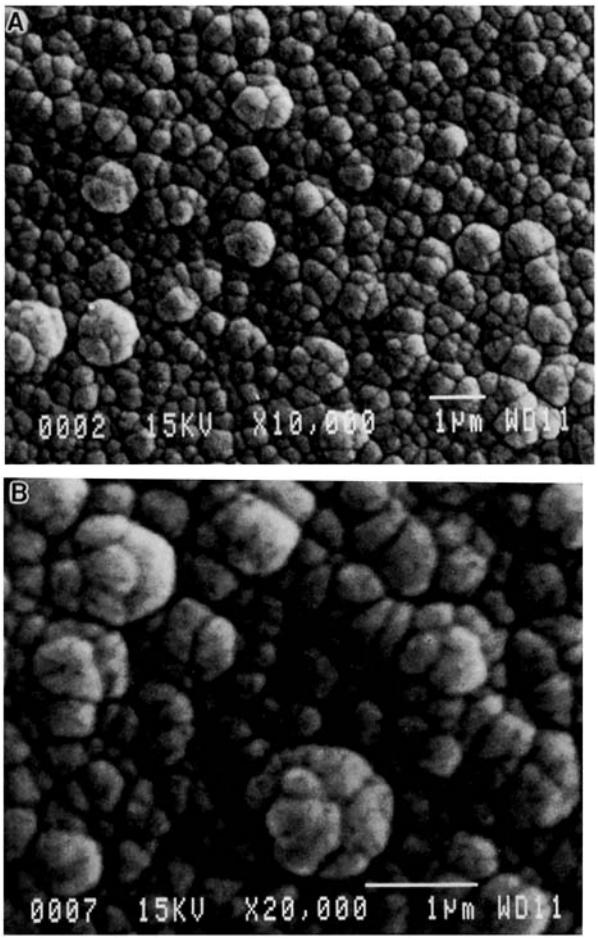

Figure 11 SEM micrographs of PPHFP: (a) lower magnification; (b) higher magnification.

CONCLUSIONS

This investigation has shown that a thin PPHFP fluoropolymer film can be readily deposited in a low temperature solvent-free process using a common industrial plasma reactor. The PP of HFP has revealed several points of interest:

1. R_p reaches a plateau at W_c, which lies between 50 and 75 W, while R_e continues to increase with power. R_d, the difference between R_p and R_e, increases at low powers, reaches a maximum at 50 W, and decreases at high powers.
2. In a monomer starved plasma R_d is unaffected by plasma exposure time and increases with F_m and P at a given power or even at a given W/F_m through a more efficient utilization of the energy supplied.
3. The density of the transparent, yellow, highly adhering PPHFP film is 2.2 g/mL, similar to those of commercial PTFE and FEP.
4. The chemical structure of PPHFP includes CF_3, CF_2, and CF groups. The abstraction of F and the preferential scission of the $C{=}CF_3$ bond can explain the significant amount of double bonds, the F/C ratio of 1.5, and the relative lack of CF_3 groups in PPHFP.
5. The PP of HFP is a gas phase dominated process that produces 0.2–0.5 μm particles. These particle are either deposited directly on the surface or agglomerate into 1-μm spheres that are then deposited on the surface. The particles and spheres are incorporated into the film with further polymerization.

The authors would like to acknowledge the support of the Israeli Ministry of Science and the Israeli Ministry of Absorption.

REFERENCES

1. D. S. Soane and Z. Martynenko, *Polymers in Microelectronics,* Elsevier, London, 1989.
2. M. T. Goosey, in *Plastics for Electronics,* M. T. Goosey, Ed., Elsevier, London, 1985, p. 319.
3. H. Yasuda, *Plasma Polymerization,* Academic Press, New York, 1985.
4. H. Biederman and Y. Osada, *Plasma Polymerization Processes,* Elsevier Science Publishers, New York, 1992.
5. H. V. Boenig, *Fundamentals of Plasma Chemistry and Technology,* Technomic Publishing, Lancaster, PA, 1988.
6. S. Morita and S. Hattori, in *Plasma Deposition, Treatment, and Etching of Polymers,* R. d'Agostino, Ed., Academic Press, New York, 1990, p. 423.
7. B. D. Ratner, A. Chilkoti, and G. P. Lopez, in *Plasma Deposition, Treatment, and Etching of Polymers,* R. d'Agostino, Ed., Academic Press, New York, 1990, p. 463.
8. S. D. Johnson, J. M. Anderson, and R. E. Marchant, *J. Biomed. Mater. Res.,* **26,** 915 (1992).
9. A. S. Hoffman, *J. Appl. Polym. Sci.; Appl. Polym. Symp.,* **42,** 251 (1988).
10. N. Inagaki, S. Tasaka, and Y. Takami, *J. Appl. Polym. Sci.,* **41,** 965 (1990).
11. Z. Takehara, Z. Ogumi, Y. Uchimoto, K. Yasuda, and H. Yoshida, *J. Power Sources,* **43–44,** 377 (1993).
12. E. Occhiello and F. Garbassi, *Polymer,* **29,** 2277 (1988).
13. S. Samukawa and S. Furuoya, *Jpn. J. Appl. Phys.—Part 2,* **32,** L1289 (1993).
14. R. d'Agostino, F. Cramarossa, F. Fracassi, and F. Illuzzi, in *Plasma Deposition, Treatment, and Etching of Polymers,* R. d'Agostino, Ed., Academic Press, New York, 1990, p. 95.
15. F. D. Egitto, V. Vukanovic, and G. N. Taylor, in *Plasma Deposition, Treatment, and Etching of Polymers,* R. d'Agostino, Ed., Academic Press, New York, 1990, p. 321.
16. M. A. Golub, T. Wydeven, and R. D. Corima, *J. Polym. Sci. A, Polym. Chem.,* **30,** 2683 (1992).

Received August 26, 1994
Accepted November 4, 1994